Activities and Modes of Action of Artificial Ion Channel Mimics

T. M. Fyles,* T. D. James, and K. C. Kaye

Contribution from the Department of Chemistry, University of Victoria, Victoria, B.C. Canada, V8W 3P6

Received July 6, 1993®

Abstract: The transport of alkali metal cations across vesicle bilayer membranes mediated by a series of 21 synthetic transporters was investigated by a pH-stat technique. The relative activities of the most active synthetic transporters were comparable to valinomycin but a factor 2–20-fold less active than gramicidin. Transport activity is controlled by structural variables; the most active materials have hydrophilic head groups, a balance of hydrophilic and lipophilic groups in the wall units, and overall length compatible with the bilayer thickness. Cation selectivity among the alkali metals, inhibition of transport by a competing cation, apparent kinetic order in transporter, and the ability of transporters to move between vesicles were determined. Significant inhibition of cation transport by competing cations, non-Eisenman selectivity patterns, and zero-order transport kinetics are proposed as criteria to recognize channel-like transporters. By these criteria, six transporters apparently act as channels, and a further four apparently act as carriers of cations. Structural variables control the mode of action of the synthetic transporters, with channel-like behavior most closely associated with columnar structures.

Natural ion transporters are large protein aggregates containing multiple transmembrane segments which act in concert to control transmembrane ion and potential gradients.[1] Structural information is now emerging from molecular biology,[2] but much of the molecular-scale detail has been inferred from low molecular weight ionophores such as gramicidin[3] or amphotericin.[4] These same sources suggest that artificial channels for the transport of ions across bilayer membranes could be designed according to the following principles: (i) a channel would have a polar core surrounded by a nonpolar exterior layer for simultaneous stabilization of an ion in transit and favorable interaction with membrane lipids and (ii) a channel would have the overall length and shape to fit into a bilayer membrane approximat ely 40 Å thick. Functional artificial ion channels have been reported which illustrate the general criteria. The most obvious course is to prepare oligopeptides with high helical content.[5] Other reported systems are based on cyclodextrin,[6] polymeric crown ether,[7] and "bouquet"-shaped crown ether and cyclodextrin motifs.[8] One of the most active systems is a simple tris-crown ether derivative reported by Gokel for the transport of sodium ion.[9] All of these systems envisage a uni- or bimolecular transmembrane structure, similar to the gramicidin structural paradigm. Alternative systems based on multicomponent aggregates, akin to an amphotericin pore, have also been explored.[10] Some time ago we reported the synthesis and activity of a functional ion channel mimic[11] and a preliminary mechanistic study[12] which suggested a channel-like behavior of one compound. A suite of 21 related materials has now been prepared,[13] and we now report a structure–activity-based elucidation of the modes of action of this class of transporters.

The design proposal, sketched in Figure 1, envisages a "core" unit lying near the bilayer mid-plane with "wall" units radiating from it. The core unit, derived from polycarboxylate crown ethers based on tartaric acid,[14] would provide a rigid framework[15] to direct the wall units to the face of the bilayer.[16] The wall units themselves would be fairly stiff to provide structural control, and would incorporate both the polar and nonpolar functionality (Y, Z) required for a channel. The structure would be completed with hydrophilic "head" groups (X) to provide overall amphiphilic

* Address correspondence to: T. M. Fyles, Department of Chemistry, University of Victoria, Box 3055, Victoria B.C., Canada V8W 3P6. Tel: 604 721 7184. Fax: 604 721 7147. Bitnet: fyles@uvvm.uvic.ca.

® Abstract published in *Advance ACS Abstracts,* December 1, 1993.

(1) (a) Houslay, M. D.; Stanley, K. K *Dynamics of Biological Membranes*; John Wiley and Sons: New York, 1982. (b) Robertson, R. N. *The Lively Membranes*; Cambridge University Press: Cambridge, 1983.

(2) (a) Betz, H. *Biochemistry* **1990**, *29*, 3591. (b) Stroud, R. M.; McCarthy, M. P.; Shuster, M. *Biochemistry* **1990**, *29*, 11009. (c) Stühmer, W. *Annu. Rev. Biophys. Biophys. Chem.* **1991**, *20*, 65.

(3) (a) Jordan, P. C. *J. Phys. Chem.* **1987**, *91*, 6582. (b) Wallace, B. A.; Ravikumar, K. *Science* **1988**, *241*, 182. (c) Langes, D. A. *Science* **1988**, *241*, 188. (d) O'Connell, A. M.; Koeppe, R. E.; Andersen, O. S. *Science* **1990**, *250*, 1256.

(4) (a) Hartsel, S. C.; Perkins, W. R.; McGarvey, G. J.; Cafiso, D. S. *Biochemistry* **1988**, *27*, 2656. (b) Bolard, J.; Legrand, P.; Heitz, F.; Cybulska, B. *Biochemistry* **1991**, *30*, 5707.

(5) (a) Sansom, M. S. P. *Prog. Biophys. Molec. Biol.* **1991**, *55*, 139 and references therein. (b) Lear, J. D.; Wasserman, Z. R.; DeGrado, W. F. *Science* **1988**, *240*, 1177. (c) Montal, M.; Montal, M. S.; Tomich, J. M. *Proc. Natl. Acad. Sci. U.S.A.* **1990**, *87*, 6929.

(6) Tabushi, I.; Kuroda, Y.; Yokota, K. *Tetrahedron Lett.* **1982**, *23*, 4601.

(7) (a) Nolte, R. J. M.; van Beijnen, A. J. M.; Neevel, J. G.; Zwikker, J. W.; Verkley, A. J.; Drenth, W. *Isr. J. Chem.* **1984**, *24*, 297. (b) Neevel, J. G.; Nolte, R. J. M. *Tetrahedron Lett.* **1984**, *25*, 2263. (c) Kragton, U. F.; Roks, M. F.; Nolte, R. J. M. *J. Chem. Soc., Chem. Commun.* **1985**, 1275.

(8) Pregel, M. J.; Jullien, L.; Lehn, J. M. *Angew. Chem., Int. Ed. Engl.* **1992**, *31*, 1637.

(9) Nakano, A.; Xie, Q.; Mallen, J. V.; Echegoyen, L.; Gokel, G. W. *J. Am. Chem. Soc.* **1990**, *112*, 1287.

(10) (a) Kunitake, T. *Proc. N. Y. Acad. Sci.* **1986**, *471*, 70. (b) Menger, F. M.; Davis, D. S.; Perischetti, R. A.; Lee, J. J. *J. Am. Chem. Soc.* **1990**, *112*, 2451. (c) Jayasuriya, N.; Bosak, S.; Regen, S. L. *J. Am. Chem. Soc.* **1990**, *112*, 5844. (d) Nagawa, Y.; Regen, S. L. *J. Am. Chem. Soc.* **1992**, *114*, 1668. (e) Fuhrhop, J. H.; Liman, U. *J. Am. Chem. Soc.* **1984**, *106*, 4643. (f) Fuhrhop, J. H.; Liman, U.; David, H. H. *Angew. Chem., Int. Ed. Engl.* **1985**, *24*, 339. (g) Fuhrhop, J. H.; Liman, U.; Koesling, V. *J. Am. Chem. Soc.* **1988**, *110*, 6840. (h) Fyles, T. M.; Kaye, K. C.; James, T. D.; Smiley, D. W. M. *Tetrahedron Lett.* **1990**, *31*, 1233. (i) Kobuke, Y.; Ueda, K.; Sokabe, M. *J. Am. Chem. Soc.* **1992**, *114*, 7618.

(11) Carmichael, V. E.; Dutton, P. J.; Fyles, T. M.; James, T. D.; Swan, J. A.; Zojaji, M. *J. Am. Chem. Soc.* **1989**, *111*, 767.

(12) Fyles, T. M.; James, T. D.; Kaye, K. C. *Can. J. Chem.* **1990**, *68*, 976.

(13) Fyles, T. M.; James, T. D.; Pryhitka, A.; Zojaji, M. *J. Org. Chem.* In press.

(14) (a) Dutton, P. J.; Fyles, T. M.; McDermid, S. J. *Can. J. Chem.* **1988**, *67*, 1097 (b) Fronczek, F. R.; Gandour, R. D.; Fyles, T. M.; Hocking, P. J.; McDermid, S. J.; Wotton, P. D. *Can. J. Chem.* **1991**, *69*, 12.

(15) (a) Fyles, T. M.; Gandour, R. D. *J. Inclusion Phenom. Mol. Recognit. Chem.* **1992**, *12*, 313. (b) Fronczek, F. R.; Gandour, R. D. In *Cation Binding by Macrocycles*; Inoue, Y., Gokel, G. W., Eds.; Marcel Dekker: New York, 1990; p 311.

(16) (a) Behr, J. P.; Lehn, J. M. *Helv. Chim. Acta* **1980**, *63*, 2112. (b) Dutton, P. J.; Fronczek, F. R.; Fyles, T. M.; Gandour, R. D. *J. Am. Chem. Soc.* **1991**, *113*, 1324.

(17) (a) Behr, J. P.; Lehn, J. M.; Vierling, P. *Helv. Chim. Acta* **1982**, *65*, 1853. (b) Desroches, J.; Dugas, H.; Bouchard, M.; Fyles, T. M.; Robertson, G. D. *Can. J. Chem.* **1987**, *65*, 1513.

0002-7863/93/1515-12315$04.00/0

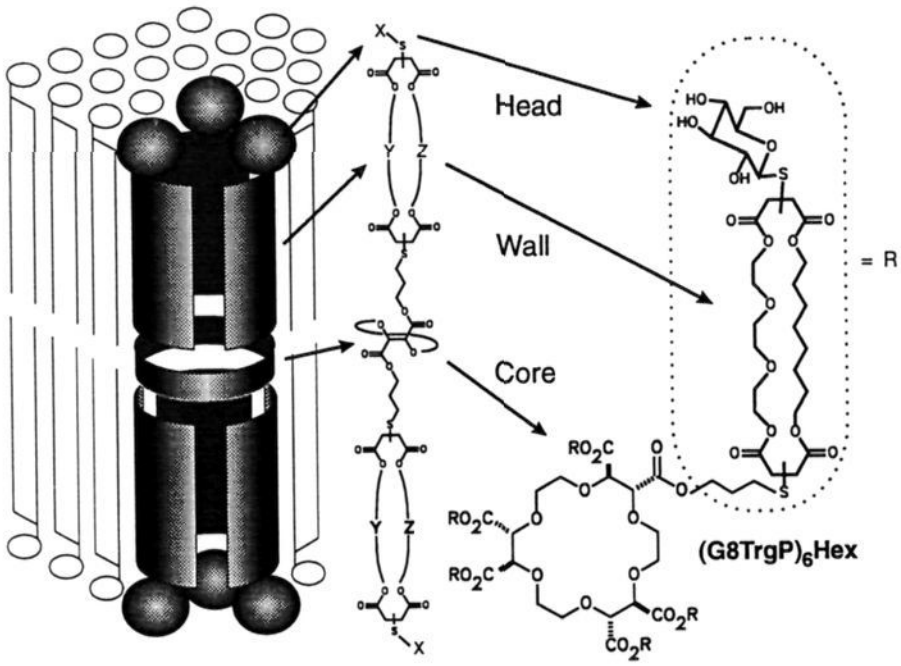

Figure 1. Design proposal for ion channel mimics.

character and to assist in the transmembrane orientation of the molecule. The wall units are based on macrocyclic tetraesters of maleic acid,[18] to provide both desired physical properties, and the synthetic advantage of facile Michael addition of the head groups.[13]

The 21 compounds of this study are indicated in Figure 2. Given the number and the complexity of these structures, we use a structurally based naming system to distinguish between similar materials. Each synthon is assigned a simple letter or number name: G = 1-mercapto-β-D-glucose, P = 3-mercaptopropyl, 8 = from 1,8-octanediol, Trg = from tris(ethylene glycol), Hex = the hexacarboxylate crown ether $18C6A_6$, etc. Each intermediate synthon is named as a combination of its synthon abbreviations with the exception that the maleate esters are implied: 8_2 = the macrocyclic tetraester from 2 mol of 1,8-octanediol, 8Trg = the macrocyclic tetraester derived from 1,8-octanediol and tris-(ethylene glycol), etc. The final names are ordered from head to core: (head + wall + spacer)$_n$ + core. Thus $(G8TrgP)_6Hex$, as illustrated in Figure 1, is (a mercapto glucose head group + a tetraester wall unit derived from 1,8-octanediol and tris(ethylene glycol) + a propyl spacer) as the hexakis ester of the $18C6A_6$ crown ether.

Figure 2 equates names and structures and provides an overview of the structural variables. The rows will illustrate the effect of variable core units, both in the number and disposition of wall units. The columns will illustrate the effect of variable wall units for a constant core. The effect of variable head group can be assessed at several core + wall intersections.

The activity of synthetic transporters in bilayer vesicles has been assessed by direct determination of transported species,[8,10,b,e-g,19] by NMR techniques,[9,20] and by visible and fluorescence spectroscopy of entrapped probe molecules.[6,7] The coupled transport of protons and cations has been assessed by use of entrapped indicators[10a,c,h,11,21] or by pH-stat techniques.[12,20b,22] The latter are well suited for a structure–activity survey and show distinctions between the behaviors of channel-forming compounds such as gramicidin and carrier compounds such as valinomycin.[12,20b] Although carriers and channels are kinetically related as extremes of a continuum,[23] they are distinct from a structure–function perspective. A carrier acts by diffusion of a cation–carrier complex through the membrane. In contrast, a channel provides a transmembrane structure to support cation diffusion. A carrier moves along with the ion; a channel is immobile relative to the moving ion. Ion channel formation is conventionally demonstrated by the observation of step conductance changes in bilayer conductivity of planar bilayers.[23] Despite the unambigous assignment of mechanism that this technique provides, it is not as well suited to a structure–activity survey as are vesicle techniques which tolerate significant variations in solution compositions. The goal of this study is to establish the structural constraints on transporter activity for any active materials. A crude sorting into "inactive", "channel-like", and "carrier-like" compounds will serve to identify candidates for detailed analysis in planar bilayers and to establish the fitness of the design proposal.

Results

Vesicles were prepared by a reverse evaporation process[24a] from an 8:1:1 mole ratio of egg phosphatidyl choline (PC)/egg phosphatidic acid (PA)/cholesterol. Lipid in ether was dispersed in a pH 6.6 buffer by sonication, the ether was removed under reduced pressure, and the vesicles were suspended in unbuffered isoosmolal choline sulfate solution. The vesicles were filtered to remove large aggregates, and the residual buffer solution was replaced by unbuffered choline sulfate solution by gel filtration. Electron microscopy[24b] showed predominantly unilamellar vesicles approximately 150-nm diameter, with some smaller unilamellar vesicles (50 nm diameter), and a small proportion of multilamellar structures (MLVs). Particle sizing by dynamic light scattering[24c]

(18) Fuhrop, J. H.; David, H. H.; Mathieu, J.; Liman, U.; Winter, H. J.; Boekema, E. *J. Am. Chem. Soc.* **1986**, *108*, 1785.
(19) Watanabe, S.; Watanabe, S.; Seno, M. *J. Membr. Sci.* **1989**, *44*, 253.
(20) (a) Ting, D. Z.; Hagan, P. S.; Chan, S. I.; Doll, J. D.; Springer, C. S. *Biophys. J.* **1981**, *34*, 189. (b) Herve, M.; Cybulska, B.; Gary-Bobo, C. M. *Eur. J. Biophys.* **1985**, *12*, 121. (c) Riddell, F. G.; Arumugam, S.; Brophy, P. J.; Cox, B. G.; Payne, M. C. H.; Southon, T. E. *J. Am. Chem. Soc.* **1988**, *110*, 734.
(21) (a) Clement, N. R.; Gould, J. M. *Biochemistry* **1981**, *20*, 1539 and 1544. (b) Whyte, B. S.; Peterson, R. P.; Hartsel, S. C. *Biochem. Biophys. Res. Commun.* **1989**, *164*, 609.
(22) Castaing, M.; Morel, F.; Lehn, J. M. *J. Membr. Biol.* **1986**, *89*, 251.
(23) (a) Läuger, P. *J. Membr. Biol.* **1980**, *57*, 163. (b) Hille, B. *Ion Channels of Excitable Membranes*; Sinauer Associates: Sunderland, MA, 1984.
(24) New, R. R. C. *Liposomes – a practical approach*; IRL Press: Oxford, 1989; (a) Chapter 2, (b) Chapter 4.1, (c) Chapter 4.2.

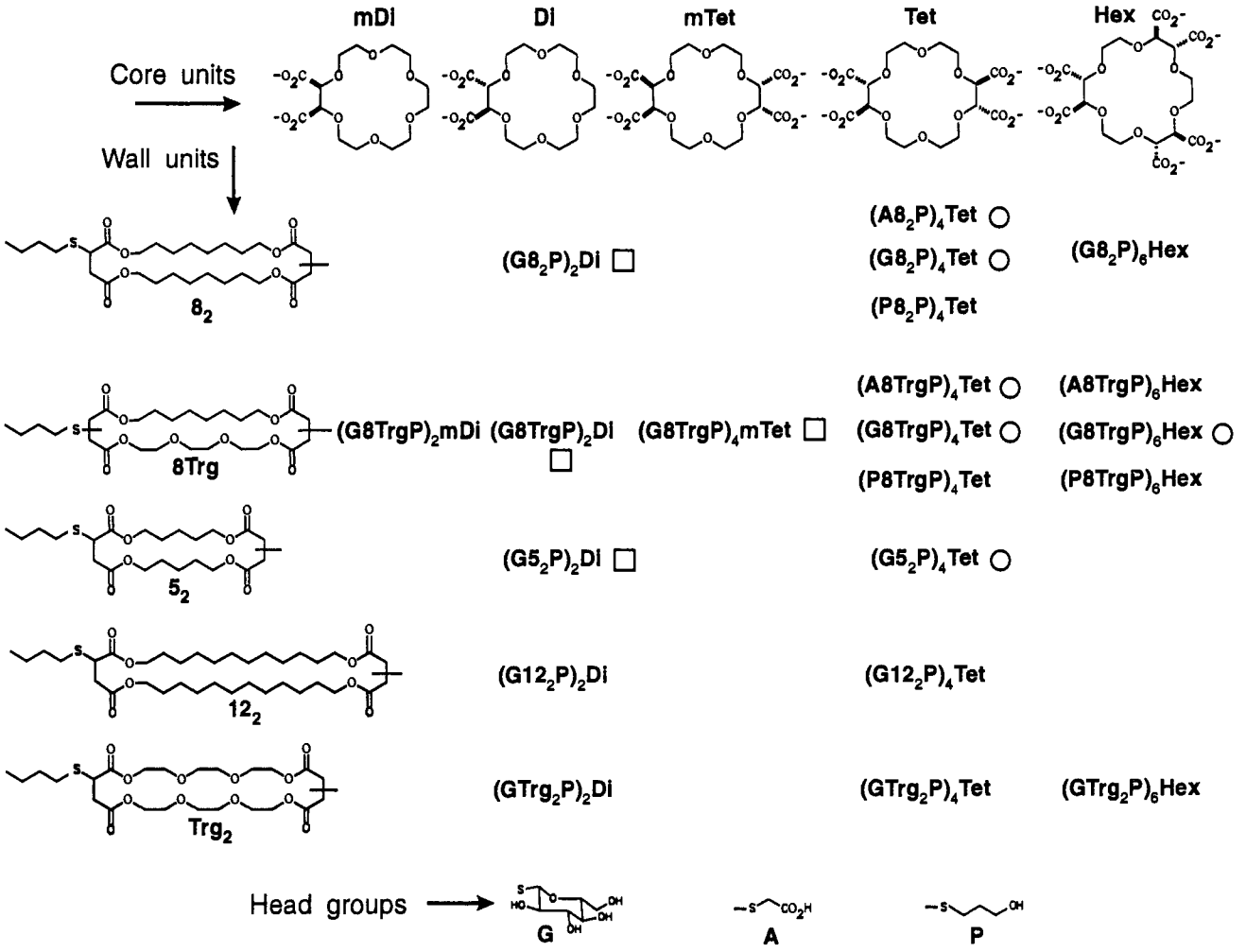

Figure 2. Structural variations and names of the transporters. All structures are composed of 2, 4, or 6 head group + wall units radiating from a core unit. Symbols indicate channel-like (○) or carrier-like (□) behavior of active materials.

subsequently confirmed a bimodal size distribution of vesicles prepared by the same technique. Vesicle solutions were stable as prepared for periods in excess of 96 h but were typically used within 24–36 h of preparation.

Aliquots of vesicle solution (1.0 mg of phospholipid, ca. 5×10^{12} vesicles) were suspended in unbuffered choline sulfate solution, and the pH was adjusted to 7.6 by addition of choline hydroxide. This is the origin of the pH-stat experimental curves illustrated in Figure 3. Addition of the proton carrier FCCP ensures that proton transport can occur rapidly.[20b] A counter gradient in alkali metal sulfate is also supported by the bilayer as the system lacks pathways for cation–proton antiport or anion–proton symport. Upon addition of a transporter, proton efflux occurs, and choline hydroxide titrant is added by the pH-stat to maintain the set pH of 7.6. The two curves of Figure 3 illustrate that the order of cation gradient creation and transporter addition is immaterial. Only when the system is fully constituted by addition of transporter does proton efflux occur. Addition of the detergent Triton X-100 at any point results in vesicle lysis with the release of any remaining entrapped buffer.

Control experiments establish the following: (1) The initial pH gradient is stable in the absence of cations for times in excess of 8 h. (2) Coupled cation/proton gradients in the presence of FCCP collapse slowly at a rate of 0.1–1 μL of titrant added per minute corresponding to a base "leakage" rate of $< 1 \times 10^{-10}$ mol $H^+ s^{-1}$. (3) The "leakage" is not accelerated by addition of solvents (methanol, THF, or DMSO) at 10 times the volumes added with the transporter solutions. (4) Lysis using Triton X-100 is very fast, but the response time of the pH-stat instrumentation limits the rate at which pH control can be reestablished. The apparent upper limit on proton efflux rate determined by this technique is $< 1.5 \times 10^{-8}$ mol $H^+ s.^{-1}$ (5) Melittin assays[25] indicate that 95% of the entrapped proton titer is contained in unilamellar vesicles (LUVs). (6) Vesicle morphology and size distribution were unaffected by transporters added at a 3-fold higher level than the highest values used in the transport experiments (typically 0.4–0.8 mol %; no changes up to 2.5 mol % transporter in lipid).

Figure 3 illustrates transport results for a single transporter ($(G8TrgP)_4Tet$) done on different days, using different vesicle preparations, and different experimental sequences. In both cases the proton efflux closely approximates a first-order process. Linear regression of log (volume added) as a function of time gives good correlation in both cases ($r^2 = 0.9975$ (top); 0.9987 (bottom)) but the rate constants differ significantly (-1.8×10^{-3} s^{-1} (top); -2.6×10^{-3} s^{-1} (bottom)). The small differences between vesicle solution entrapment efficiency, lipid concentration, and buffering capacity on the outside of the vesicles translates to initial volume differences (4.88 mL (top); 4.57 mL (bottom)), to initial transporter concentration differences (0.62×10^{-6} M (top); 0.66×10^{-6} M (bottom)), and to different Triton X-100 lyse volumes (0.461 mL = 1.83×10^{-6} mol H^+ entrapped (top); 0.445 mL = 1.77×10^{-6} mol H^+ entrapped (bottom)). As previously,[12,20b,22] the extent of transport varies between the two experiments; neither one reaches the "limit" of 95% based on the MLV content of the solutions. The apparent initial proton efflux rate can be derived from the first-order rate constant and the apparent "infinity" value for the experiment ($rate_0 = k$ (infinity volume choline hydroxide concentration)). This gives initial rate values for the

(25) Bhakoo, M.; Birkbeck, T. H.; Freer, J. H. *Can. J. Biochem. Cell. Biol.* **1985**, *63*, 1.

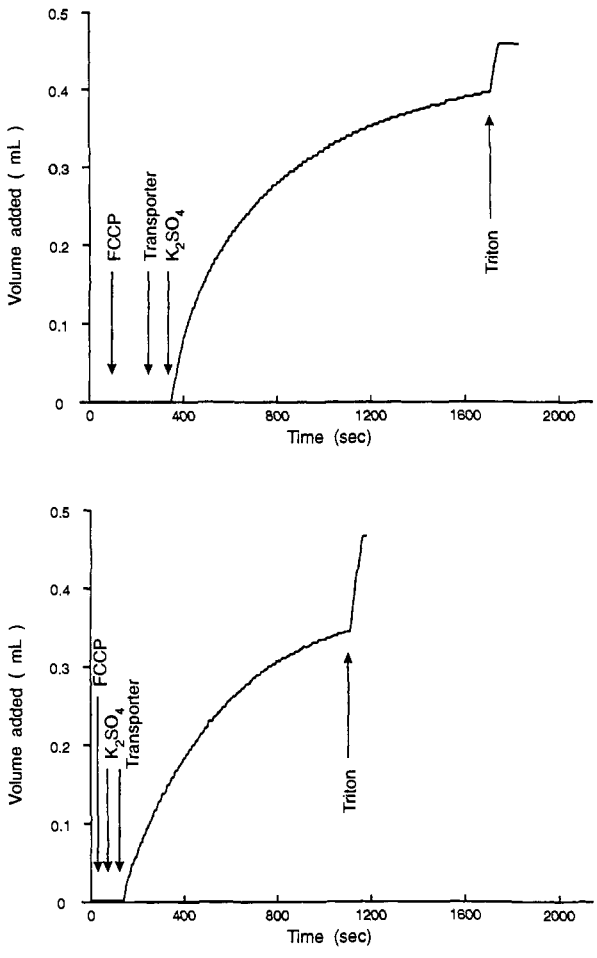

Figure 3. Experimental pH-stat curves of volume of choline hydroxide titrant added as a function of time, illustrating "first-order" behavior for the transporter (**G8Trgp**)$_4$Tet. Details of the experiment are discussed in the text.

two experiments of 3.2×10^{-9} and 3.8×10^{-9} mol H^+ s^{-1} for the top and bottom experiments, respectively. These rates differ by 8% for experiments with transporter concentrations which differ by 6%. Reproducibility between different vesicle preparations is estimated to be ±10%. Replicates within a single vesicle preparation can be better than ±5%. Experiments involving a range of concentrations were done using a single vesicle preparation to improve precision.

Figure 4 shows another common type of experimental result, distinct from the "first-order" behavior illustrated in Figure 3. The "zero-order" evolution of volume with time gave the apparent initial rate of proton efflux directly by linear regression (8.2×10^{-10} mol H^+ s^{-1} for Figure 4). Active transporters showed either "zero-order" or "first-order" behavior; mixed cases were not found. Highly active "zero-order" transporters showed a linear evolution volume with time for the first 75–85% of the total transport event, followed by a rapid leveling during the final stages of transport. Zero- and first-order behaviors do not merge into one another as a function of experimental conditions (transporter concentration, cation concentration, or type).

The activity of the suite of compounds (Figure 2) is summarized in Table I. The apparent kinetic order in transporter was determined from the variation in rate as a function of transporter concentration.[26] The values are all less than unity, indicating that extensive aggregation does not occur.[27] Normalization to a transporter concentration of 2×10^{-6} M included correction for the apparent kinetic order determined. A first-order dependence

(26) Fyles, T. M.; Malik-Diemer, V. A.; McGavin, C. A.; Whitfield, D. M. *Can. J. Chem.* **1982**, *60*, 2259.
(27) Fyles, T. M.; Tweddell, J. Unpublished results.

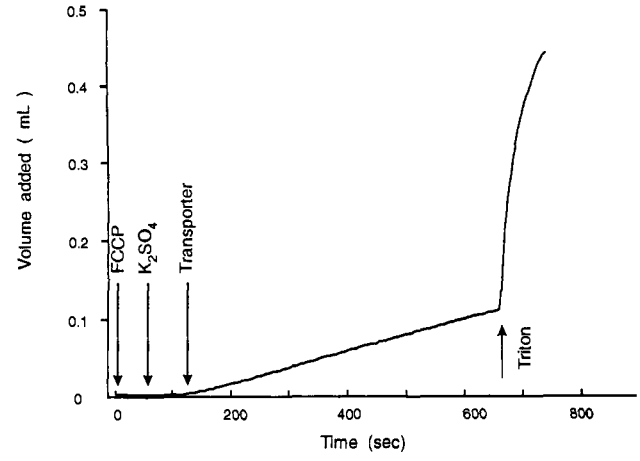

Figure 4. Experimental pH-stat curves of volume of choline hydroxide titrant added as a function of time, illustrating "zero-order" behavior for the transporter (**G8$_2$p**)$_4$Tet at a concentration of 3.2×10^{-7} M. Other conditions as given in Table I.

on transporter concentration was assumed for the least active compounds. The normalized rates give a rough separation of the most active and least active materials and support semiquantitative analysis. The most active materials are a factor of 2–20 less active than gramicidin but are comparable to valinomycin. The least active materials are a factor of 50–100 less active than gramicidin, indicating that indiscriminate damage to bilayers does not occur. Some subunits are well represented in the lower activity group: the P head group (3-hydroxypropyl), the long wall unit 12_2, and the lipophilic wall group Trg_2 occur only near the bottom of Table I. Unconnected subunits are inactive at concentrations equivalent to the covalent compounds. For example, while (G8TrgP)$_4$mTet is very active at 1.2×10^{-6} M, the hexaene (8TrgP)$_4$mTet, and the parent crown ether mTet are both inactive at the same concentration. The wall unit terminated as an alcohol (G8TrpPOH), the simpler wall unit 8TrgPOH, and the mercaptoglucose head group are inactive at 8×10^{-6} M.

Table II presents data on the rates of cation transport of alkali metal sulfates by the most active materials. Each row was determined using a single vesicle preparation, so differences greater than ±5% are significant. Marked selectivity differences are observed, particularly between the strongly Na^+ selective (G8TrgP)$_4$Tet and the K^+ selective isomer (G8TrgP)$_4$mTet. Some selectivity patterns are given in Figure 5, relative to the Na^+ transport rate in each case. The "peak" selectivity observed in some cases is the Eisenman III/IV selectivity sequence typical of many crown ether cation complexes.[28] The Na^+ selective patterns of (G8TrgP)$_4$Tet, (A8$_2$P)$_4$Tet, (A8TrgP)$_4$Tet, and possibly (A8TrgP)$_6$Hex are not related to any Eisenman selectivity sequence, indicating that equilibrium ion binding considerations do not govern the rate-limiting transport process in these cases.[28]

Transport of one cation can in some cases be inhibited by another cation;[12] the data is presented in Table III. Separate consecutive experiments from a single vesicle preparation are compared so a rate ratio <0.95 indicates significant inhibition, and a ratio >1.05 indicates significant acceleration. A carrier mechanism could result in rate enhancement but could not give rise to inhibition.[29] The observation of significant inhibition is therefore a strong indication of channel formation.

A Michaelis–Menten analysis of the variation in rate as a function of K^+ concentration[27] (Lineweaver–Burke plot) gave the following values ($V_{max} \times 10^9$ mol H^+ s^{-1}, $K_m \times 10^3$ M: gramicidin, 4.0 ± 0.6 and 4.1 ± 0.4; valinomycin, 0.6 ± 0.2 and 36 ± 8; (G8TrgP)$_4$Tet, 4.4 ± 0.4 and 3.8 ± 0.6; (G8$_2$P)$_4$Tet, 3.6

(28) Eisenman, G. *Ion Selective Electrodes*, Durst, R. A., Ed.; NBS Special pub. 314. NBS: Washington, 1969; Chapter 1.
(29) Behr, J. P.; Kirch, M.; Lehn, J. M. *J. Am. Chem. Soc.* **1985**, *107*, 241. Fyles, T. M. *Can. J. Chem.* **1987**, *65*, 884.

Table I. Ranked Transport Activities of Compounds Surveyed[a]

transporter	[Tr] × 10^6, M	rate × 10^9, mol H^+ s^{-1}	kinetic order[e]	normalized rate[f] × 10^9, mol H^+ s^{-1}	extent of transport %[g]
gramicidin	0.25	6.6[b]	0.39 ± 0.07	14.9	56
$(G8trgP)_4Tet$	0.66	3.8[b]	0.66 ± 0.08	8.2	84
$(G8TrgP)_4mTet$	1.20	4.4[b]	0.76 ± 0.04	6.5	81
$(G8_2P)_2Di$	1.54	4.9[b]	0.66 ± 0.05	5.8	83
valinomycin	1.01	2.6[b]	0.50 ± 0.07	3.6	*h*
$(G8TrgP)_2Di$	1.81	1.9[b]	0.98 ± 0.05	2.1	83
$(G8_2P)_4Tet$	1.62	1.6[c]	0.43 ± 0.02	1.8	*h*
$(A8TrgP)_4Tet$	2.56	2.1[b]	0.76 ± 0.09	1.7	43
$(A8_2P)_4Tet$	2.07	1.7[c]	0.21 ± 0.07	1.7	*h*
$(G5_2P)_2Di$	3.25	2.2[b]	0.73 ± 0.02	1.6	71
$(G8TrgP)_6Hex$	1.40	1.0[b]	0.87 ± 0.09	1.3	47
$(G5_2P)_4Tet$	1.26	0.8[b]	0.95 ± 0.04	1.1	60
$(G8_2P)_6Hex$	2.00	0.8[c]	*i*	0.8	*h*
$(G8TrgP)_2mDi$	2.04	0.7[b]	*i*	0.7	65
$(GTrg_2P)_2Di$	2.20	0.5[b]	*i*	0.4	94
$(P8TrgP)_4Tet$	1.39	0.3[b]	*i*	0.4	93
$(GTrg_2P)_6Hex$	3.45	0.5[b]	*i*	0.3	49
$(A8TrgP)_6Hex$	3.16	0.4[c]	*i*	0.3	*j*
$(G12_2P)_4Tet$	3.11	0.3[c]	*i*	0.2	*j*
$(P8TrgP)_6Hex$	3.08	0.3[b]	*i*	0.2	7
$(GTrg_2P)_4Tet$	2.22	*d*	*d*	*d*	<5
$(G12_2P)_2Di$	3.04	*d*	*d*	*d*	<5
$(P8_2P)_4Tet$	2.37	*d*	*d*	*d*	<5

[a] Transport across vesicle bilayer membranes at 298 K in the presence of (1.5–1.8) × 10^{-7} M FCCP and (4.7–4.9) × 10^{-2} M K_2SO_4. [b] Determined from first-order rate analysis, see text. [c] Determined from zero-order rate analysis, see text. [d] No transport detected; rate <1 × 10^{-10} mol H^+ s^{-1}. [e] Transport across vesicle bilayer membranes at 298 K in the presence of (1.5–1.8) × 10^{-7} M FCCP and (4.7–4.9) × 10^{-2} M K_2SO_4. Variable [Tr] in the range (0.3–3.5) × 10^{-6} M; slope of log (rate) as a function of log ([Tr]) ± statistical error, $r^2 > 0.98$ on >3 points in all cases. [f] Normalized to [Tr] = 2 × 10^{-6} M; normalized rate = (2 × 10^{-6}/[Tr])$^{\text{kinetic order}}$ × rate. [g] Expressed as percent of the total amount of entrapped H^+ assessed by Triton lysis. [h] Transport occurred to the MLV limit. [i] Not determined; normalized rate calculation assumes kinetic order = 1. [j] Full extent of transport not determined.

Table II. Transport of Alkali Metal Cations by Active Transporters[a]

transporter	[Tr] × 10^6, M	rate × 10^9, mol H^+ s^{-1}					
		Li^+	Na^+	K^+	Rb^+	Cs^+	none
$(G8TrgP)_4Tet$[b]	0.51	0.4	9.5	2.9	4.4	4.5	0.0
$(G8TrgP)_4mTet$[b]	0.57	0.0	0.9	4.8	4.3	1.8	
$(G8_2P)_2Di$[b]	1.03	0.0	2.0	3.7	3.5	2.8	
$(G8TrgP)_2Di$[b]	1.82	0.0	1.1	1.9	1.9	1.5	0.0
$(G8_2P)_4Tet$[c]	1.62	0.2	1.6	1.8	1.9	1.4	
$(A8TrgP)_4Tet$[b]	2.41	0.3	2.7	1.8	2.5	2.5	0.4
$(A8_2P)_4Tet$[c]	2.02	0.4	4.1	2.7	2.8	3.1	
$(G5_2P)_2Di$[b]	3.42	1.0	1.9	2.2	2.6	1.1	
$(G8TrgP)_6Hex$[b]	2.03	0.5	1.4	4.0	2.5	2.0	0.0
$(G5_2P)_4Tet$[b]	1.33	0.2	0.6	0.8	0.8	0.6	0.0
$(A8TrgP)_6Hex$[c]	3.16	0.2	0.5	0.4	0.6	0.7	

[a] Transport across vesicle bilayer membranes at 298 K in the presence of (1.5–1.8) × 10^{-7} M FCCP and (4.7–4.9) × 10^{-2} M M_2SO_4 (4.9 × 10^{-2} M choline sulfate for "none"). [b] Determined from a first-order analysis, see text. [c] Determined from a zero-order analysis, see text.

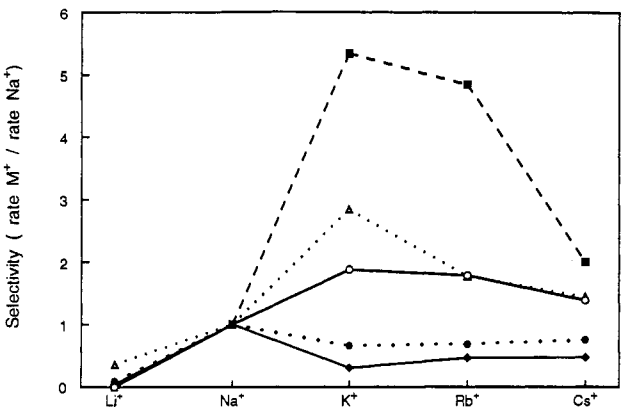

Figure 5. Selectivity patterns relative to Na^+ derived from the data in Table II: $(G8TrgP)_4mTet$ (■), $(G8TrgP)_6Hex$ (△), $(G8_2P)_2Di$ (○), $(A8_2P)_4Tet$ (●), $(G8Trg)_4Tet$ (◆).

± 0.2 and 1.3 ± 0.3; $(G8TrgP)_6Hex$, 2.5 ± 0.3 and 5.6 ± 0.8). These data show considerable variation in the Michaelis constant K_m, with smaller variation in the maximal rate V_{max}. The V_{max} for the carrier valinomycin is significantly lower than the V_{max} for gramicidin, consistent with expectation.[23]

Table IV summarizes "migration" experiments, one of which is illustrated in Figure 6. This experiment probes the ability of a transporter to migrate between vesicles through the aqueous phase. The experiment begins as previously discussed, but before the transporter is added, half the solution is withdrawn from the cell (point A). The remaining solution is treated with the transporter, and proton efflux occurs. As the plateau is reached, the fresh vesicle solution containing no transporter is returned to the cell. Any subsequent transport which occurs indicates that the transporter can migrate through the aqueous phase. The rates in the two sections can be determined as previously explained. The second rate can also be predicted from the first rate, the dilution factor, and the apparent kinetic order (n) previously determined ($rate_2 = rate_1 \times ([Tr]_2/[Tr]_1)^n$). Table IV reports a migration ratio defined as the ratio of the experimental $rate_2$ to the expected value of $rate_2$. A high migration ratio is consistent with facile transfer of transporter between vesicles, as previously observed with valinomycin.[20b] Conversely, a low migration ratio indicates that the transporter is bound to the vesicles, as observed with gramicidin.[20b]

Discussion

The control experiments, the spectrum of activities, and the contrasting selectivity patterns observed established that this suite of compounds form cation transporting pathways which are controlled by structural variables. The compounds do not indiscriminately damage vesicles by a detergent-like action, nor do they act via aggregate structures or clusters of transporter in the bilayer opening defects adjacent to the additive. The latter mechanism shows an apparent kinetic order greater than one in the same vesicle system.[30]

(30) Fyles, T. M.; Kaye, K. C.; Pryhitka, A.; Tweddell, J.; Zojaji, M. *J. Supramol. Chem.* In press.

Table III. Inhibition of Active Transporters by Competing Cations[a]

transporter	[Tr] × 10^6, M	M_1	M_2	rate × 10^9, mol H^+ s^{-1}	rate ratio[d]
$(G8TrgP)_4Tet^b$	0.63	Na^+		5.9	
	0.62	Na^+	K^+	2.7	0.46
$(G8TrgP)_4mTet^b$	0.58	K^+		3.5	
	0.57	K^+	Li^+	3.6	1.02
$(G8_2P)_2Di^b$	1.03	K^+		4.0	
	1.00	K^+	Li^+	4.1	1.04
$(G8TrgP)_2Di^b$	3.03	K^+		2.5	
	2.98	K^+	Li^+	2.8	1.13
$(G8_2P)_4Tet^c$	3.19	K^+		1.8	
	3.13	K^+	Li^+	1.8	0.97
$(A8TrgP)_4Tet^b$	2.44	Na^+		2.7	
	2.39	Na^+	Li^+	2.4	0.88
$(A8_2P)_4Tet^c$	2.05	Na^+		3.8	
	2.01	Na^+	Li^+	2.8	0.75
$(G5_2P)_2Di^b$	3.25	K^+		2.2	
	3.36	K^+	Li^+	2.3	1.02
$(G8TrgP)_6Hex^b$	2.05	K^+		1.7	
	1.98	K^+	Li^+	1.3	0.76
$(G5_2P)_4Tet^b$	0.63	K^+		2.9	
	0.65	K^+	Li^+	2.3	0.78

[a] Transport across vesicle bilayer membranes at 298 K in the presence of (1.5–1.8) × 10^{-7} M FCCP and (4.7–4.9) × 10^{-2} M $(M_1)_2SO_4$ (and (0.9–1.0) × 10^{-2} $(M_2)_2SO_4$). [b] Rate determined from a first-order analysis, see text. [c] Rate determined from a zero-order analysis, see text. [d] Ratio of (rate with M_1 and M_2 present/(rate with M_1 alone).

The first-order evolution of the pH-stat volume added with time has been previously rationalized by a mechanism in which gramicidin channel opening is rate-limiting, followed by very rapid equilibration of the vesicle contents with the external solution.[20b] This explanation is consistent with the very high conductivity of gramicidin channels in planar bilayer membranes[3] and with the slow migration of gramicidin between vesicles as studied by NMR.[20d] A first-order pH-stat curve for the carrier valinomycin is consistent with diffusion-limited transport with a decrease in rate reflecting a decrease in gradient.[29] The extent of transport in either case is related to the migration ability of the transporter. Transporters such as valinomycin can equilibrate all vesicles simultaneously by migration throughout the whole vesicle population, while transporters with lower migration ability act primarily against the fraction of vesicles initially attacked.[20b] The same explanations are relevant in the examples presented here, with the added complexity of a range of transporter migration abilities, rather than just the limiting cases represented by gramicidin and valinomycin.

The zero-order transport behavior observed in some cases indicates that the transporter is not responding to the internal concentration of the vesicle and hence does not behave as a carrier. The rate must depend only on the number of vesicles remaining with ion gradients. The experimental result is inconsistent with the "all-or-nothing" process described above, but is consistent with a process where partial equilibration of vesicles contents with the external medium would occur during a short channel-opening event. Several channel openings are apparently required to completely equilibrate the vesicle contents. Vesicles appear to equilibrate equally, at a rate that depends only on the random openings of ion channels. The difference between a first-order and a zero-order channel mediated process is related to the lifetime of the channel opening or to the efficiency of ion transport. Neither aspect can be directly probed in this system, and further progress depends on study of channel conductivity and gating in planar bilayers.

The experiment involves partitioning between the aqueous and lipid phases, which might vary considerably across the series of compounds. Similar, but more highly oxygenated, "bouquet" molecules are partitioned to vesicle membranes, and the extent varies with the nature of the head group.[31] Unfavorable partition is a likely explanation for the poor performance of compounds containing the Trg_2 wall unit. The migration ratios also suggest that penetration of the bilayer is relatively efficient for most compounds in this series. Zero-order transport could conceivably reflect very poor partitioning to the lipid phase. However, higher concentrations would force more transporter into the lipid and would shift toward first-order behavior. This was not observed.

If the rate-limiting processes are related to channel gating and carrier diffusion, the experiments on cation selectivity, apparent kinetic order, and Michaelis–Menten parameters are only indirect probes of the ion translocation steps. Channel-like behavior is most strongly indicated by significant inhibition of ion transport by a competing ion. If observed, zero-order transport and/or a non-Eisenman selectivity sequence are also suggestive of channel-like behavior. The inhibition and selectivity criteria together indicate that $(G8TrgP)_4Tet$, $(A8_2P)_4Tet$, and $(A8TrgP)_4Tet$ are channel-like. On the basis of the inhibition results alone, $(G8TrpP)_6Hex$ and $(G5_2P)_4Tet$ can be added to this group, while the zero-order criterion includes $(G8_2P)_4Tet$ as a channel-like transporter. Conversely, active materials with significant enhancement of rate by a competing ion and a regular Eisenman selectivity pattern are more likely to be carriers. These criteria suggest that $(G8TrgP)_4mTet$, $(G8TrgP)_2Di$, and probably $(G5_2P)_2Di$ and $(G8_2P)_2Di$ are carriers. These conclusions are indicated by the symbols adjacent to the names on Figure 2: an open circle (○) for channel-like behavior, and a box (□) for carrier-like behavior.

Conclusions

The main goal of this study was to establish that structural control could lead to control of transporter activity. The range of transport activities, selectivities, and mechanistic distinctions observed confirm that structural control is possible. Moreover, some active "lead" compounds have been identified for further investigation by more refined mechanistic probes.

The structural control of transport mode of action is evident from the clustering of the symbols on Figure 2. Probable carriers are found among the derivatives of the Di core unit, while channel-like transporters are derivatives of the Tet and Hex core units. The wall units 8_2, 8Trg, and 5_2 are suitable for either mode of action, but a balance of lipophilic character is essential for active materials.

The case of the isomers Tet and mTet is particularly instructive. The marked conformational preference for an *anti* relationship between the carboxylate groups, if translated to the transporter molecule as a whole, would give columnar structures similar to those depicted in Figure 1 for Tet derivatives, but would give Y-shaped structures for derivatives of mTet.[14] The marked differences between the isomeric transporters $(G8TrgP)_4Tet$ and $(G8TrgP)_4mTet$ must be related to the basic conformational differences, implying a very strong structural control.

Experimental Section

Materials. Egg phosphatidylcholine and egg phosphatidic acid (egg PC and egg PA) were purchased from Avanti Polar Lipids, Inc., Pelham, AL. Bis-Tris (2,2-bis(hydroxymethyl)-2,2',2''-nitrilotriethanol), carbonyl cyanide–[(trifluoromethoxy)phenyl]hydrazone (FCCP), cholesterol, choline hydroxide (20% in water), gramicidin D, melittin, and valinomycin were obtained from Sigma/Aldrich; sulfuric acid (ultrapure) was obtained from Fluka. Only D^3 (deionized, double-distilled) water was used. The preparation and purification of the transporters used is reported separately.[13]

A. Choline Sulfate.[22] Choline hydroxide (250 mL of 20% solution in 500 mL of D^3 water) was titrated to pH 6.5 with concentrated sulfuric

(31) Jullien, L.; Lazrak, T.; Canceill, J.; Lacombe, L.; Lehn, J.-M. *J. Chem. Soc., Perkin Trans. 2* **1993**, 1011.
(32) Menger, F. M.; Lee, J.-J.; Aikens, P.; Davis, S. *J. Colloid Interface Sci.* **1989**, *129*, 185.

Table IV. Migration of Active Transporters between Vesicles[a]

transporter	$[Tr]_1 \times 10^6$, M	$[Tr]_2 \times 10^6$, M	$rate_1 \times 10^9$, mol H^+ s^{-1}	$rate_2 \times 10^9$, mol H^+ s^{-1}	expected $rate_2$[b] $\times 10^9$, mol H^+ s^{-1}	ratio[c]
gramicidin	0.35	0.18	6.5	0.43	5.0	0.09
$(G8TrgP)_4Tet$	1.06	0.53	2.7	1.0	1.7	0.58
$(G8TrgP)_4mTet$	1.07	0.62	4.3	2.7	2.8	0.95
$(G8_2P)_2Di$	1.97	1.03	4.2	1.8	2.7	0.66
valinomycin	2.01	1.05	3.1	2.3	2.2	1.03
$(G8TrgP)_2Di$	2.05	1.05	1.6	0.85	0.83	1.02
$(G8_2P)_4Tet$	3.04	1.61	1.6	0.43	1.2	0.35
$(A8TrgP)_4Tet$	3.86	2.05	1.6	0.89	1.0	0.90
$(A8_2P)_4Tet$	2.05	1.21	1.6	0.90	1.43	0.63
$(G5_2P)_2Di$	5.10	3.25	4.0	2.7	2.9	0.94
$(G8TrgP)_6Hex$	6.42	3.39	4.8	0.44	2.7	0.16
$(G5_2P)_4Tet$	1.26	0.7	0.78	0.26	0.47	0.55

[a] Transport across vesicle bilayer membranes at 298 K in the presence of $(1.5–1.8) \times 10^{-7}$ M FCCP and $(4.7–4.9) \times 10^{-2}$ M K_2SO_4. Vesicle solution (2.5 mL) was removed before transporter was added. Rates determined from a first-order analysis. [b] Rate calculated from observed $rate_1$ and apparent kinetic order; see text. [c] Ratio of (experimental value of $rate_2$)/(expected value of $rate_2$), see text.

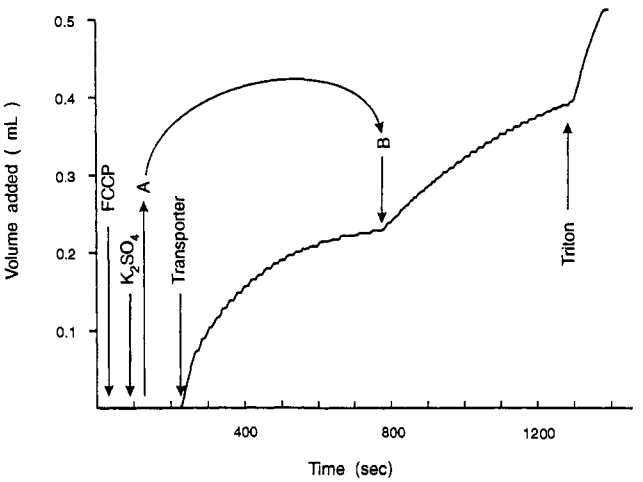

Figure 6. Experimental pH-stat curves of volume of choline hydroxide titrant added as a function of time, illustrating a migration experiment for the transporter **(G8TrgP)$_4$Tet**, see Table IV. Vesicle solution (2.5 mL), removed at point A, was returned to the cell at point B.

acid and decolorized with activated charcoal, and the solution was concentrated to a thick oil by rotary evaporation. Residual water was removed by azeotropic drying with absolute ethanol, and crystalline choline sulfate was obtained from absolute ethanol/ether at −10 °C for 16 h (2 crops). Combined batches were dried for 24 h in vacuum.

Solutions. A. Internal buffer solution: 0.20 M Bis-Tris, and 0.054 M D-mannitol; pH adjusted to 6.60 using 0.45 M H_2SO_4. **B. External solution**: 0.110 M choline sulfate, and 0.093 M D-mannitol; cold storage under nitrogen and periodic filtration through Millipore GS 0.22-μm filters was required to stabilize the solution. **C. Lipid stock solution**: 8:1:1 (molar ratio; 16:2:1 weight ratio) of egg PC/egg PA/cholesterol in $CHCl_3$ at a concentration of 50 mg of PC per 3 mL. The solution was stored under nitrogen at −15 °C shielded from light. **D. Choline hydroxide titrant**: 4.75 mM cholien hydroxide, 0.35 M D-mannitol; base titer established versus potassium hydrogen phthalate. FCCP, gramidicin D, and valinomycin were dissolved in methanol to concentrations of 9.6×10^{-4}, 3.3×10^{-5}, and 2.8×10^{-3} M, respectively. Triton X-100 was diluted by a factor of 20 with D^3 water. The transporters were dissolved in methanol at concentrations between 8.2×10^{-4} and 5.70×10^{-3} M.

Vesicle Preparation. Mixed lipids (3 mL of stock solution containing 50 mg of PC) were evaporated onto the walls of a boiling tube (20 mm dia, 50 mm deep, B24 joint), and the lipid film was dried for 4 h at 50 °C under vacuum. The dried lipids were dissolved in anhydrous ether (6 mL) and 2 mL of internal buffer was added. The mixture was sonicated to an opalescent single phase using a Heat Systems W385 Ultrasonic probe sonicator (13-mm tip; 40 2-s pulses at 50% duty cycle and 50% power output). The ether was removed from the mixture by slow rotary evaporation at 150–200 mmHg pressure with a bath temperature of 25 °C. As the ether begins to evaporate, the solution coats the sides of the flask. A gradual decrease in pressure over 5 min to a pressure of 100–150 mmHg promotes spontaneous bubbling which continues for about 5 min. Spontaneous bubbling must be controlled (via pressure) to give small bubbles at an early stage and larger bubbles at a later stage. The mixture goes through a gelatinous phase and then becomes a freely flowing liquid which is held at 100 mmHg pressure for 20 min. External buffer solution (3 mL) is added, and the remaining ether is removed by rotary evaporation for 15 min at a pressure of 50 mmHg. The vesicles were "sized" through Nucleopore filters (1 μm followed by 0.4 μm) using nitrogen pressure. Excess buffer components were removed by gel filtration (Sephadex G-25M, PD-10 column, Pharmacia). The column was equilibrated with external solution, the "sized" vesicle mixture was added (2.5–4 mL), and the column was eluted with external solution. The first 0.5 mL of cloudly eluent after the exclusion volume (2.5 mL) were discarded. A total of 3–4 mL of eluent containing vesicles was retained. The prepared vesicles were used within 36 h.

Vesicle Characterization. Total phospholipid in the vesicle preparations (typically $(1.0–1.3) \times 10^{-2}$ M) was determined by colorimetric analysis of a phosphomolybdate complex of the head groups. Vesicle morphology was assessed by transmission electron microscopy (phosphotungstic acid stain[24b]). Quantitative size distribution analysis of vesicles by dynamic light scattering was performed using a NICOMP C370 submicron particle sizer.[32] Vesicle entrapment of buffer solution is directly determined by the pH-stat experiment (Triton lysis). The fraction of multilamellar vesicles (MLVs) was assessed from the proportion of the vesicle contents released by a single aliquot of melittin.[29]

pH-stat Experiment. The pH-stat system used a Metrohm 655 Dosimat burette and thermostated (25 °C) titration cell controlled by a Metrohm 614 Impulsomat and Metrohm 632 pH-meter, fitted with a glass electrode and a standard calomel electrode linked to the cell via an electrolyte bridge to give the following: calomel‖0.11 M choline sulfate, 0.093 M mannitol‖vesicles in 0.11 M choline sulfate, 0.039 M mannitol at a set pH‖glass electrode. The burette was linked to an HP-85 microcomputer for data acquisition of time versus volume curves.

A. Typical Procedure. External solution (3.8 mL) and vesicles (0.2 mL) were mixed in the cell. A pH gradient was imposed by addition of choline hydroxide titrant solution to a set pH of 7.60 (ca. 0.4 mL). FCCP (9.6×10^{-4} M in methanol, 10 μL) was added, followed by typically 0.5 mL of a cation sulfate salt solution (0.5 M) to create an opposing cation gradient. The transporter ($(0.8–5.7) \times 10^{-3}$ M in methanol, 2–50 μL) was added, and the pH and cation gradients began to collapse. The order of addition of cation sulfate and transporter can be reversed. Volume of base added versus time data was accumulated until rate of addition fell to below 1–2 μL/min. The remaining entrapped protons were released by lysis of the vesicles with Triton X-100 and were subsequently titrated. The data were analyzed as described in the text.

Acknowledgment. The ongoing support of the Natural Sciences and Engineering Research Council of Canada is gratefully acknowledged.

Supplementary Material Available: A listing of the experimental rates determined leading to the data presented in Tables II–IV (10 pages). This material is contained in many libraries on microfiche, immediately follows this article in the microfilm version of the journal, and can be ordered from the ACS; see any current masthead page for ordering information.